International Symposium on District Heating and Cooling, Nottingham Trent University, 17th Edition, 6–9 September 2021, Nottingham, United Kingdom

A case study on using district heating network flexibility for thermal load shifting

Tijs Van Oevelen[a,b,*], Luca Scapino[a,b], Jad Al Koussa[a,b], Dirk Vanhoudt[a,b]

[a]*VITO, Boeretang 200, 2400 Mol, Belgium*
[b]*EnergyVIlle, Thor Park 8310, 3600 Genk, Belgium*

Abstract

In district heating (DH) systems, the time of use of energy is becoming more important. For example, the use of sustainable baseload units over peak units is favored. Also heat production units coupled to the electricity grid, such as cogeneration plants and heat pumps, can profit from fluctuating prices and balance the electricity network at the same time. In this context, DH utility companies can benefit from shifting thermal loads in time. In the H2020 TEMPO project, a case study is being conducted to shift thermal loads using the thermal flexibility of the DH network. The thermal storage capacity of the network is utilized by dynamically changing the supply temperature. The study consists of two experimental campaigns, designed to dynamically characterize the available storage capacity in the DH network. In these campaigns, the supply temperature in one of the TEMPO demo sites was increased/decreased several times per day. The flow rate, supply and return temperatures were measured at the heat source and at a large customer building. The analysis of the experimental results focused on two aspects: the propagation of flow temperatures through the network and the response of customer substations to supply temperature changes. The data and knowledge gathered in these test campaigns will be used to develop models for a model predictive controller (MPC) which will be tested in the next heating season.

Keywords: thermal networks flexibility; supply temperature response tests; substation response tests; experimental campaign

1. Introduction

In the coming years and decades, EU member states will face ambitious challenges to increase energy efficiency and the use of renewable energy, and to reduce greenhouse gas emissions. The decreasing energy demand from buildings due to increased energy efficiency is putting pressure on the economic viability of district heating (DH) networks [1-3]. Furthermore, the volatile fossil fuel prices in recent years have introduced uncertainty in fuel expenses for DH network operators [4-5]. This uncertainty is considered a high risk, hindering the investment in new DH networks.

Nevertheless, this challenge can be overcome if two key modifications can be introduced to traditional networks. Firstly, heat losses in the network should be reduced. Secondly, the share of renewable or waste heat sources should be increased in DH networks [6-7]. This can be achieved by reducing the temperature levels in the network, and by adding flexibility in the network to cope with the volatile and uncontrollable character of sustainable energy sources. Energy flexibility can be defined as the ability to shift energy flows in time to accommodate operational constraints and objectives [8]. The importance of flexibility is expected to further increase together with the penetration of intermittent renewable energy sources. In district heating systems, the traditional source of flexibility is in the form of a central thermal storage tank at the heat production site. In recent years, also demand-side management of customer heat demand has received considerable attention as an alternative or complimentary source of flexibility [8-13]. Another alternative is the use of the thermal storage capacity in the piping of the thermal network. The idea is to

* Corresponding author. Tel.: +32 14335152
E-mail address: tijs.vanoevelen@vito.be

increase the supply temperature of the network when renewable heat is available, and to reduce it again when there is a lack of heat from a renewable source. In this way, the network pipes are used as a thermal storage buffer, as an alternative or complementary to hot water storage tanks. Especially in large networks, this could represent a substantial amount of storage capacity [8, 14], which could be used to shift heat loads in time. In fact, district heating utility operators have been using this thermal network flexibility already for decades when preloading the network pipes to prepare for peak heat demands. This was highlighted by Fredriksen et al. [15] and Basciotti et al. [16] who describe how a limited amount of heat or cold can be stored temporarily by raising or lowering the temperature of the water in the thermal network, allowing for a certain degree of peak heat demand shaving. Also, Laakkonen et al. [17] presented a controller that optimizes the supply temperature in order to reduce the heat load peaks by charging or discharging the network pipes.

Moreover, Merket et al. [18], Jiang et al. [19] and Benonysson et al. [20] provided methods and examples for optimal control and scheduling of Combined Heat and Power (CHP) plants using the thermal inertia of the grid for thermal storage. A number of other publications also focused on the optimization of supply temperatures such as Leśko et al. [21] where the focus was on modelling DH systems for operational optimization, with special focus on thermal energy storage in the DH pipelines; and Giraud et al. [22] that developed new advanced control method for DH systems with a focus on exploiting the thermal storage capacity of the network and optimizing between pumping energy and heat losses.

Nevertheless, to the knowledge of the authors, systematic use of thermal network flexibility has not yet been realized by an automated real-time supervisory control system. The work presented here prepares for the development of a model predictive controller able to achieve this. It is performed within the Horizon 2020 TEMPO ('TEMPerature Optimisation for Low Temperature District Heating across Europe') project [23], in which six technical innovations are developed, customized and implemented in district heating networks:

1. An automatic on-line supervision ICT platform, able to detect and diagnose sub-optimally behaving building substations.
2. Visualization tools for experts (to support monitoring and analyzing network behavior) and non-expert users (to give insight in their energy use, to suggest energy saving actions).
3. Smart DH network controller to balance supply and demand and to minimize the return temperature. This controller is an extension of the controller developed in the Horizon 2020 STORM project [24].
4. An innovative piping system, including a third recirculation pipe to avoid high return temperatures from substations because of comfort reasons.
5. Fault detection methodologies for building heating systems that often deliver return temperatures higher than expected.
6. Decentralized buffers at the consumer side to reduce peak heat demands in rural DH networks.

These technologies are demonstrated in two demo sites. One demo site is a newly built network supplying heat to about 100 new single-family houses, located in Windsbach, in the rural area near Nuremberg, Germany. The second demo site is the existing DH network in Brescia, Italy.

Concretely, this paper describes the results of two test campaigns to determine the behavior of the DH network and the building substations, necessary to build and train the models used by the controller. Section 2 includes the methodology, describing the demo site, the experimental setup and the test plans. Then, in section 3, the results of the two test campaigns are presented and discussed. The final section 4 includes the conclusions and an outlook to the further work

2. Methodology

2.1. Demo site

The demo site is located in the city of Brescia, Northern Italy, and consists of a peripheral branch of the existing high temperature (up to 130 °C) DH system operated by "A2A Calore e Servizi". It is the largest DH network in Italy, with more than 1 TWh annual supply, covering about 70% of the city's heat demand, and 60% of the heat is produced by a waste-to-energy plant. The portion of the branch used for demonstration provides heat for space heating and domestic hot water (DHW) preparation in a residential area in the southern part of the city. The demo site includes 35 customers: one large multi-family house (MFH) and 34 single-family terraced houses, with a total contract capacity of about 700 kW.

This site was selected considering also the large replicability potential, since it is representative for many European DH networks. To perform the tests without directly affecting the whole branch in the DH system, it was necessary to decouple the demo site from the rest of the branch. Therefore, new supply and return pipes were laid and a local subnetwork that can be independently operated was created, using a mixing station (MS). The mixing station mixes the hot water from the main network with the return from the demo site (the ratio depends on the ambient temperature) to get a colder supply to the demo site. Sensors to monitor the water supply and return temperatures were installed as well as indoor temperature sensors in some buildings. Moreover, hardware tools communicating with a cloud were placed to transmit the data and enable the smart control.

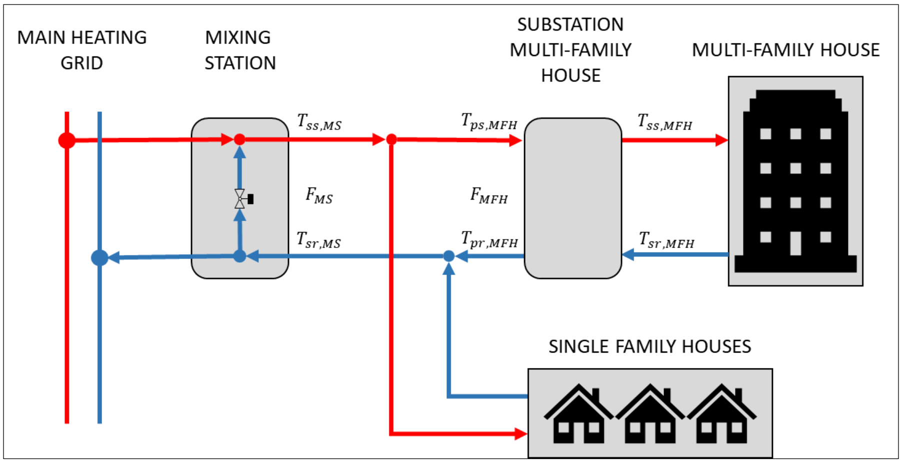

Fig. 1. Conceptual scheme showing the temperatures (T) and flow rates (F) recorded at the demo site. [NOTE TO PUBLISHER: this figure contains color.]

In Fig. 1, a conceptual scheme of the demo site is shown, with the main flows and temperatures recorded during the experimental campaign and used in the current analysis. The data collected consisted mainly of temperature and flow meters readings, at variable frequency in the range of 10–30 minutes. This frequency depended also on the communication between the sensors and the router. Sometimes communication issues led to data gaps, especially during the first experimental campaign. The resulting datasets have been resampled with a 10 minutes frequency for the data analysis. At the MS secondary side (i.e. after mixing), the flow rate (F_{MS}), supply ($T_{ss,MS}$) and return temperatures ($T_{sr,MS}$) were recorded. At the substation, supply and return temperatures were recorded on both the primary ($T_{ps,MFH}$, $T_{pr,MFH}$) and secondary ($T_{ss,MFH}$, $T_{sr,MFH}$) sides while the flow rate (F_{MFH}) was recorded only on the primary side.

2.2. Test Plan

The experimental campaigns consist of varying the supply temperature at the secondary side of the mixing station ($T_{ss,MS}$) and monitoring how this variation propagates through the network. During these response tests, two main approaches were used to set $T_{ss,MS}$, and they are conceptually shown in Fig. 2.

The first approach consists of selecting two supply temperature values, $T_{ss,MS,low}$ and $T_{ss,MS,high}$, and setting the MS supply temperature to one of the two values. This approach has the main advantage of having only two temperature levels that can be easily identified during the postprocessing of the data. A disadvantage is that if the outdoor temperature changes considerably during the experimental campaign, the two fixed temperature levels can become unsuitable. If the outdoor temperature decreases excessively, it can be that $T_{ss,MS,low}$ is too low for the customers' heat demand to be satisfied, and the customers' substations would reach their maximum flow rate. If the outdoor temperature increases too much, it can be that $T_{ss,MS,high}$ cannot be reached because the supply temperature on the primary side of the main heating grid, which is among others determined by the outdoor temperature, is below $T_{ss,MS,high}$.

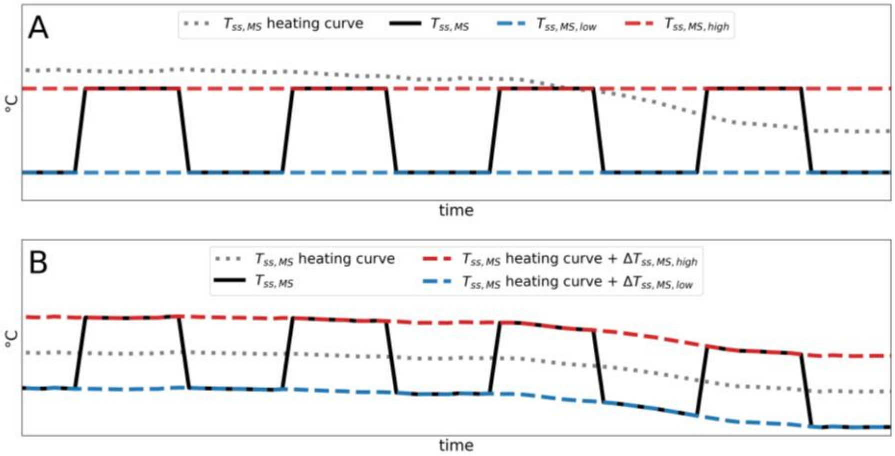

Fig. 2. Conceptual presentation of two approaches for setting supply temperature form mixing station: (A) test approach with fixed high and low supply temperature of the mixing station; (B) test approach with high and low supply temperature of the mixing station determined relative to the mixing station heating curve. See Fig. 1 for symbol nomenclature. [NOTE TO PUBLISHER: this figure contains color.]

The second approach consists of setting two MS supply temperature offsets, $\Delta T_{ss,MS,low}$ and $\Delta T_{ss,MS,high}$, with respect to the heating curve instead of having two fixed values. This approach dynamically sets the mixing station supply temperature considering the heating curve during the experimental campaign. This second approach substantially reduces the risk of unsuitable supply temperature setpoints that may occur due to an abrupt change in weather conditions, because it stays closer to normal operation.

During the first experimental campaign the first approach was used, and for the second experimental campaign, the second approach was used due to its advantages with rapidly changing weather conditions. In Fig. 3, the test plan of the two campaigns is shown. The first experimental campaign was performed during three weeks in December 2020. During the first and third week, the supply temperature was increased from 80 °C ($T_{ss,MS,low}$) to 95 °C ($T_{ss,MS,high}$) during long pulses of three hours, three times per day. During the second week, short one-hour pulses were performed four times per day.

The second experimental campaign consisted of a three-hours pulse in the night and three two-hour pulses during the day, during one week in February 2021. All the temperature pulses consisted of increasing by 15 °C the supply temperature with respect to the heating curve values ($\Delta T_{ss,MS,low}$ = 0 °C, $\Delta T_{ss,MS,high}$ = 15 °C).

<table>
<tr><th>Begin</th><th>End</th><th></th><th>00:00</th><th>00:30</th><th>01:00</th><th>01:30</th><th>02:00</th><th>02:30</th><th>03:00</th><th>03:30</th><th>04:00</th><th>04:30</th><th>05:00</th><th>05:30</th><th>06:00</th><th>06:30</th><th>07:00</th><th>07:30</th><th>08:00</th><th>08:30</th><th>09:00</th><th>09:30</th><th>10:00</th><th>10:30</th><th>11:00</th><th>11:30</th><th>12:00</th><th>12:30</th><th>13:00</th><th>13:30</th><th>14:00</th><th>14:30</th><th>15:00</th><th>15:30</th><th>16:00</th><th>16:30</th><th>17:00</th><th>17:30</th><th>18:00</th><th>18:30</th><th>19:00</th><th>19:30</th><th>20:00</th><th>20:30</th><th>21:00</th><th>21:30</th><th>22:00</th><th>22:30</th><th>23:00</th><th>23:30</th></tr>
<tr><td rowspan="2">30/11/2021</td><td rowspan="2">20/12/2021</td><td>1st campaign short pulses</td><td colspan="10">80°C</td><td colspan="2">04:45-05:45 (95°C)</td><td colspan="8">80°C</td><td colspan="2">10:00-11:00 (95°C)</td><td colspan="6">80°C</td><td colspan="2">14:00-15:00 (95°C)</td><td colspan="8">80°C</td><td colspan="2">19:00-20:00 (95°C)</td><td colspan="8">80°C</td></tr>
<tr><td>1st campaign long pulses</td><td colspan="6">80°C</td><td colspan="6">02:45-05:45 (95°C)</td><td colspan="8">80°C</td><td colspan="6">10:00-13:00 (95°C)</td><td colspan="12">80°C</td><td colspan="6">19:00-22:00 (95°C)</td><td colspan="4">80°C</td></tr>
<tr><td>15/02/2021</td><td>21/02/2021</td><td>2nd campaign</td><td colspan="4">+0°C</td><td colspan="6">01:45-04:45 (+15°C)</td><td colspan="8">+0°C</td><td colspan="4">09:00-11:00 (+15°C)</td><td colspan="6">+0°C</td><td colspan="4">14:00-16:00 (+15°C)</td><td colspan="6">+0°C</td><td colspan="4">19:00-21:00 (+15°C)</td><td colspan="6">+0°C</td></tr>
</table>

Fig. 3. Test plan of the experimental campaigns. [NOTE TO PUBLISHER: this figure contains color.]

3. Results

3.1. First experimental campaign – December 2020

In Fig. 4, the supply and return temperatures and flow rates measured at the MS and at the MFH are shown for the test day of 14/12/2020. It can be seen that the MS supply temperature $T_{ss,MS}$ reacts as expected, following the control signal ($T_{ss,MS,ctrl}$). During the night (22:00–05:00), the MFH is not consuming energy for space heating and the flow rate is low. At 5:00, the heating system turns on, and the flow rates sharply increase both at the MFH and at the MS.

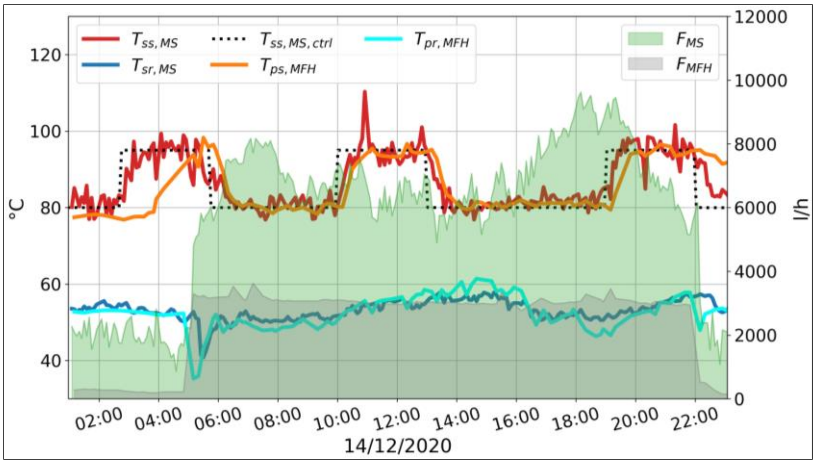

Fig. 4. Test day: 14/12/2020. Supply ($T_{ss,MS}$, $T_{ps,MFH}$) and return ($T_{sr,MS}$, $T_{pr,MFH}$) temperatures, mixing station supply temperature control signal ($T_{ss,MS,ctrl}$), and flow rates (F_{MS}, F_{MFH}) at the mixing station and at the multi-family house. See Fig. 1 for meaning of symbols. [NOTE TO PUBLISHER: this figure contains color.]

During the day time, the MFH flow rate is relatively constant, while the MS flow rate varies with peaks around 7:00 and 18:00. These variations are driven by the heating demand of the single-family houses connected to the network. Regarding the propagation of the supply temperature from the mixing station to the MFH, it can be seen how the flow rate determines the delay between the two locations. During the night-time temperature pulse starting at 2:45, the supply temperature change at the MS is propagated to the MFH with a delay of a little more than one hour. During the day-time pulses, the delay is approximately 10 to 20 minutes. The time delays are in agreement with the flow transit times, which are about 1 hour during night time and about 20 minutes during day time based on pipe segment lengths and average flow rates.

Concerning the return temperatures, at 05:00 there is a sharp return temperature decrease at the MFH, which is then propagated to the MS with a delay of approximately 20 minutes. The reason is that, initially, the thermal energy in the hot water is being transferred to the components of the hydraulic circuit such as radiators, pipes, heat exchangers, etc. that cooled down during the night.

In Fig. 5, the primary and secondary supply temperature at the MFH substation are shown together with the substation secondary-side supply temperature setpoint ($T_{ss,MFH,set}$), which varies depending on the outdoor temperature using a heating curve. During the daily supply temperature pulses, it was expected that the MFH substation controller would react by lowering the flow rate F_{MFH}. However, it remained approximately constant with small variations within the range of 3000–3500 l/h. The reason was that the MFH flow rate was almost always at its maximum value because the substation secondary-side supply temperature setpoint ($T_{ss,MFH,set}$) of approximately 60 °C could not be reached, according to the measurements ($T_{ss,MFH}$). This was probably due to the too low supply temperature on the primary side of the substation ($T_{ps,MFH}$), which was not set based on the heating curve but following the approach in Fig. 2A. For this reason, in the following campaign, the mixing station supply temperature control signals were set with respect to the heating curve (approach in Fig. 2B).

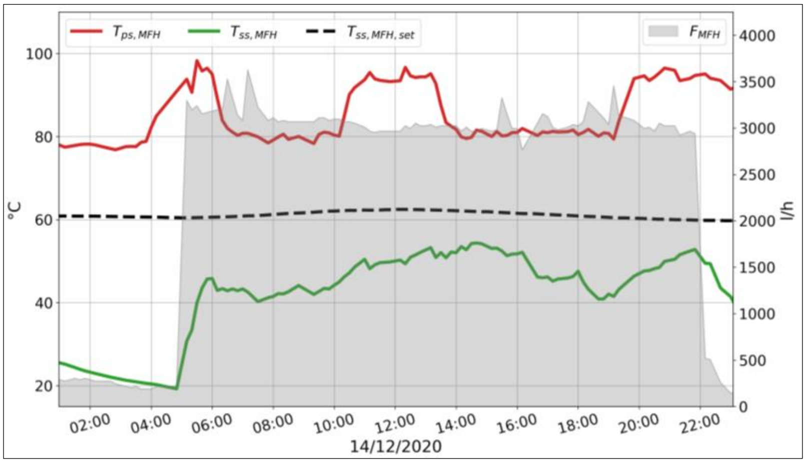

Fig. 5. Test day: 14/12/2020. Primary ($T_{ps,MFH}$) and secondary ($T_{ss,MFH}$) supply temperatures, secondary supply temperature setpoint ($T_{ss,MFH,set}$), and primary flow rate (F_{MFH}) at the substation of the multi-family house. See Fig. 1 for meaning of symbols. [NOTE TO PUBLISHER: this figure contains color.]

3.2. Second experimental campaign – February 2021

In the second campaign, the aim was to obtain the expected substation primary flow rate variation in response to a change in the MS secondary-side supply temperature. The supply temperature pulses were planned to follow the approach in Fig. 2B, which took into consideration the heating curve and, consequently, the outdoor temperature. Fig. 6 shows the temperatures and flow rates at the MS and at the MFH for the test day of 19/02/2021. Regarding the supply temperature propagation, similar considerations to Fig. 4 can be made.

The return temperature behavior in the night is different from the first experimental campaign. The reason is that, in this experimental campaign, the heating system could turn on during night-time, thereby avoiding warming up the hydraulic circuit at the beginning of the morning peak. At 1:30, F_{MFH} has a first slight increase, indicating that water starts to circulate in the heating system circuit, and it starts to warm up the system components as well. The return temperature, which results from the mixing between the return temperature from the DHW circuit and the space heating circuit, decreases due to the increasing space heating flow rate fraction, which is colder at the system start up.

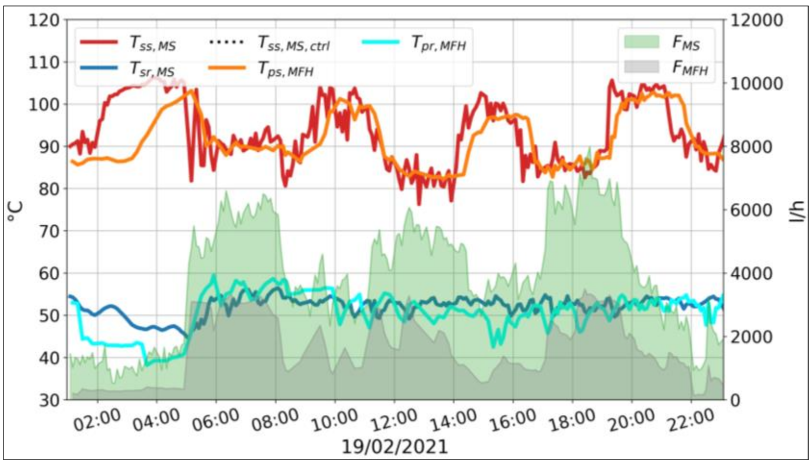

Fig. 6. Test day: 19/02/2021. Supply ($T_{ss,MS}$, $T_{ps,MFH}$) and return ($T_{sr,MS}$, $T_{pr,MFH}$) temperature, mixing station supply temperature control signal ($T_{ss,MS,ctrl}$), and flow rates (F_{MS}, F_{MFH}) at the mixing station and at the multi-family house. See Fig. 1 for meaning of symbols. [NOTE TO PUBLISHER: this figure contains color.]

At 3:30 the flow rate has a second slight increase, lowering further the return temperature at the substation. At 5:00 the morning peak starts, and the return temperature starts to increase because, contrarily to the test day in Fig. 4, the hydraulic circuit components have been already heated up.

At the MFH substation (Fig. 7), this time it was possible for the secondary-side supply temperature $T_{ss,MFH}$ to reach its setpoint value $T_{ss,MFH,set}$. Consequently, the flow rate at the MFH varies during the day as a result of feedback control, reacting to the primary-side supply temperature pulses as expected. An increase of supply temperature on the primary side $T_{ps,MFH}$ leads to a decrease in the primary-side flow rate F_{MFH}, and vice versa, in order to provide a specific heating power to the customers. This effect on the flow rate provides a potential for heat load shifting. When the supply temperature is increased, the ΔT increases temporarily from 30 °C to 45 °C. This leads to a corresponding 50% increase in heat load, which is stored in the network. Afterwards, when the supply temperature drops back but the flow rate is still reduced, this amount of energy is discharged again.

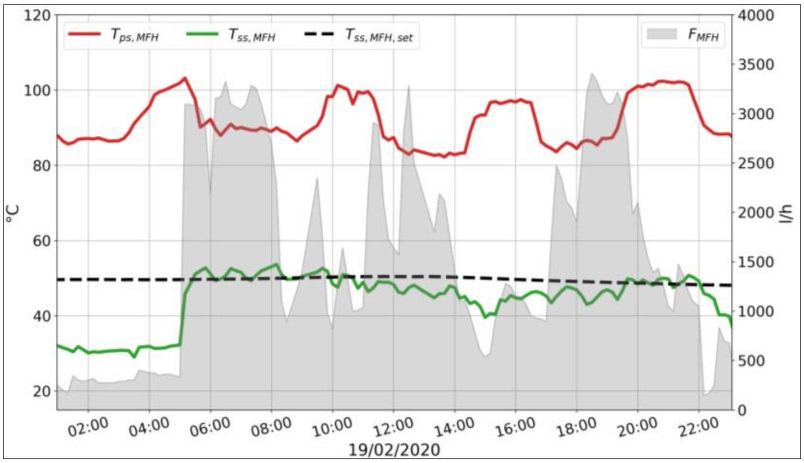

Fig. 7. Test day: 19/02/2021. Primary ($T_{ps,MFH}$) and secondary ($T_{ss,MFH}$) supply temperatures, secondary supply temperature setpoint ($T_{ss,MFH,set}$), and primary flow rate (F_{MFH}) at the substation of the multi-family house. See Fig. 1 for meaning of symbols. [NOTE TO PUBLISHER: this figure contains color.]

4. Conclusions and future work

During the experimental campaigns, the supply temperature at the MS was varied several times per day. The flow rates, supply and return temperatures were recorded both at the MS at the MFH substation. In the first experimental campaign in December 2020, the supply temperature was varied between two fixed temperature levels. The results showed that the supply temperature propagated from the MS to the MFH substation within a time range varying from twenty minutes during the day, to just over one hour during the night when the MS flow rate is much lower. Moreover, the MFH substation was not responding as expected to supply temperature variations because it was not able to reach its secondary-side supply temperature setpoint. The reason was that the supply temperature at the MS was not high enough, and the flow rate on the primary side was always close to its maximum, with small fluctuations during the day.

In the second experimental campaign in February 2021, the supply temperature at the MS was dynamically varied based on a heating curve value and fixed temperature offsets. The results showed that the MFH substation was able to reach its setpoint and reacted as expected to supply temperature variations on the primary side. During a supply temperature increase, the flow rate on the primary side decreased, and vice versa.

Furthermore, night-time setback of the MFH space heating system was present during the first experimental campaign while it has been removed during the second campaign. With night-time setback, the return temperature on the primary side of the MFH substation had a sharp decrease in the morning when the heating system is turned on. The reason was that, initially, the hot water had to warms up all the heating system components as well, and this can lead to a power peak. During the second experimental campaign, the heating system was on also during the night thereby preventing a sharp return temperature decrease during the morning start up.

The first results of the experimental campaign were presented in this paper. Based on the data collected, further work will focus on the development of models for a smart controller, using the flexibility offered by the DH network pipes. The aim is to develop this controller in the coming months, and to test it in the next heating season.

Acknowledgements

This work has been carried out in the TEMPO project, funded by the European Union's Horizon 2020 programme under grant agreement 768936. The authors would like to thank Christian Johansson from NODA Intelligent Systems AB and Ilaria Marini from A2A Calore e Servizi S.r.l. for their support.

References

[1] Henrik Lund, Bernd Möller, Brian Vad Mathiesen, et al. The role of district heating in future renewable energy systems, Energy, 2010, 35 (3), 1381-1390.
[2] Marie Münster, Paul Erik Morthorst, Helge V. Larsen, et al. The role of district heating in the future Danish energy system, Energy, 2012, 48 (1), 47-55.
[3] David Connolly, Henrik Lund, Brian Vad Mathiesen, et al. Heat Roadmap Europe: Combining district heating with heat savings to decarbonise the EU energy system, Energy Policy, 2014, 65, 475-489.
[4] Florian Kienzle, Peter Ahčin, Göran Andersson. Valuing Investments in Multi-Energy Conversion, Storage, and Demand-Side Management Systems Under Uncertainty, IEEE Trans. Sustainable Energy, 2011, 2(2), 194-202.
[5] Scott Kelly, Michael Pollitt. An assessment of the present and future opportunities for combined heat and power with district heating (CHP-DH) in the United Kingdom, Energy Policy, 2010, 38 (11), 6936-6945.
[6] Henrik Lund, Paul Alberg Østergaard, Miguel Chang, et al. The status of 4th generation district heating: Research and results. Energy, 2018 164, 147-159.
[7] Henrik Lund, Sven Werner, Robin Wiltshire, et al. 4th Generation District Heating (4GDH). Integrating smart thermal grids into future sustainable energy systems. Energy, 2014, 68, 1-11.
[8] Annelies Vandermeulen, Bram van der Heijde, and Lieve Helsen. Controlling district heating and cooling networks to unlock flexibility: A review. Energy, 151:103-115, May 2018.
[9] Elisa Guelpa, Ludovica Marincioni, Stefania Deputato, Martina Capone, Stefano Amelio, Enrico Pochettino, and Vittorio Verda. Demand side management in district heating networks: A real application. Energy, 182:433-442, Sep. 2019.
[10] Costanza Saletti, Mirko Morini, and Agostino Gambarotta. The status of research and innovation on heating and cooling networks as smart energy systems within horizon 2020. Energies, 13(11):2835, Jun. 2020.
[11] Annelies Vandermeulen, Ina De Jaeger, Tijs Van Oevelen, Dirk Saelens, and Lieve Helsen. Analysis of building parameter uncertainty in district heating for optimal control of network flexibility. Energies, 13(23):6220, Nov. 2020.
[12] Simone Buffa, Mohammad Hossein Fouladfar, Giuseppe Franchini, Ismael Lozano Gabarre, and Manuel Andrés Chicote. Advanced control and fault detection strategies for district heating and cooling systems-a review. Applied Sciences, 11(1):455, Jan. 2021.
[13] Tijs Van Oevelen, Dirk Vanhoudt, Christian Johansson, Ed Smulders. Testing and performance evaluation of the STORM controller in two demonstration sites. Energy, 197, 117177, 2020.
[14] Annelies Vandermeulen, Tijs Van Oevelen, Bram van der Heijde, and Lieve Helsen. A simulation-based evaluation of substation models for network flexibility characterization in district heating networks. Energy, 201:117650, Jun. 2020.
[15] Frederiksen Svend, Werner Sven. District heating and cooling. chapter 10. Studentlitteratur; 2013. p. 469-81.
[16] D. Basciotti, F. Judex, O. Pol, and R.-R. Schmidt. Sensible heat storage in district heating networks: a novel control strategy using the network as storage. In Conference proceedings of the 6th international conference on renewable energy storage conference IRES, 2011.
[17] Leo Laakkonen, Timo Korpela, Jyri Kaivosoja, Matti Vilkko, Yrjö Majanne, and Maria Nurmoranta. Predictive supply temperature optimization of district heating networks using delay distributions. Energy Procedia, 116:297-309, Jun. 2017.
[18] Lennart Merkert, Ashvar Haime, and Sören Hohmann. Optimal scheduling of combined heat and power generation units using the thermal inertia of the connected district heating grid as energy storage. Energies, 12(2):266, Jan. 2019.
[19] Yibao Jiang, Can Wan, Audun Botterud, Yonghua Song, and Shiwei Xia. Exploiting flexibility of district heating networks in combined heat and power dispatch. IEEE Transactions on Sustainable Energy, 11(4):2174-2188, Oct. 2020.
[20] A. Benonysson, B. Bøhm, and H. F. Ravn. Operational optimization in a district heating system. Energy Conversion and Management, 36(5):297-314, 1995.
[21] Michal Leśko and Wojciech Bujalski. Modeling of district heating networks for the purpose of operational optimization with thermal energy storage. Archives of Thermodynamics, 38(4):139-163, Dec. 2017.
[22] Loïc Giraud, Massinissa Merabet, Roland Baviere, and Mathieu Vallée. Optimal control of district heating systems using dynamic simulation and mixed integer linear programming. In Proceedings of the 12th International Modelica Conference, Prague, Czech Republic, May 15-17, 2017. Linköping University Electronic Press, Jul. 2017.
[23] TEMPO project – Towards a sustainable future for district heating. Available online: https://www.tempo-dhc.eu
[24] STORM project – Developing an innovative District Heating & Cooling (DHC) network controller to increase the use of waste heat and renewable energy sources and boost energy efficiency at district level. Available online: https://www.storm-dhc.eu.